IMPLEMENTATION AND IMPROVEMENT OF INDOOR WEARABLE UWB/INS INTEGRATION POSITIONING METHOD

Zongbo Liao [1], Zhenqi Zheng[2], You Li[2,3*]

[1] Electronic Information School, Wuhan University, Wuhan, China - liaozb@whu.edu.cn
[2] State Key Laboratory of Information Engineering in Surveying, Mapping and Remote Sensing, Wuhan University, Luoyu Road, Wuhan, China - (liyou, zhengzhenqi)@whu.edu.cn
[3] Hubei Luojia Laboratory, Wuhan, China

Commission IV, WG IV/5

KEY WORDS: UWB, INS, Kalman Filter, Positioning, DOP.

ABSTRACT:

Aiming at the problem that the Ultra-Wide-Band (UWB) positioning accuracy is reduced in the Non-Line-of-Sight (NLOS) environment, a UWB positioning accuracy evaluation mechanism is introduced. This paper analyzes the geometric distribution of UWB equipment theoretically to evaluate the positioning accuracy of the UWB system. Furthermore, it optimizes the geometric distribution of UWB and optimizes the UWB positioning algorithm model to improve the positioning accuracy. A set of UWB positioning accuracy estimation process is proposed. Through theoretical analysis and simulation, a model of the influence of the geometric distribution of base stations on the UWB positioning precision is established. The obtained model provides a reference for setting and adjusting the measurement noise in the Kalman filter for UWB/Inertial Navigation System (INS) integration positioning, which improves the combined positioning accuracy.

1. INTRODUCTION

Outdoor positioning technology based on Global Navigation Satellite System (GNSS) or GNSS/ Inertial Navigation System (INS) integration has been successfully applied and commercialized (Balland, 2012). However, in indoor areas, the availability of GNSS signals can be poor or even unavailable. Therefore, additional sensors are required to achieve indoor positioning (Poulose et al., 2019). The algorithms currently used for indoor positioning mainly include geometric positioning, dead reckoning, database matching, and their integration. Among them, geometric positioning, especially distance-based multilateration, is the most commonly used method.

Most indoor positioning solutions now use wireless technologies such as WIFI, ZigBee, and Ultra-Wide-Band (UWB). Among them, UWB has the characteristics of low power consumption, large bandwidth, high-speed communication, high time resolution, high data rate, and short wavelength (Park and Rappaport, 2007). Thus, this paper chooses UWB as a part of the positioning solution. A challenge for UWB positioning is that its ranging precision and maximum measuring distance will be significantly reduced due to the influence of Non-Line-of-Sight (NLOS) and multipath. Therefore, this paper adopts the integrated positioning system of UWB/INS to improve the positioning precision. Once initialized, the INS can provide independent navigation without the need to receive external signals or interact with the external environment. This feature ensures navigation continuity and reliability when UWB performance is degraded by NLOS or multipath effects (El-Sheimy and Li Y, 2021).

This paper will build a personnel positioning platform based on UWB/INS integration and implement the corresponding Extended Kalman Filter (EKF) algorithm for wearable application scenarios. On this basis, performance improvements are made for the difficulties in practical applications. Aiming at the challenge of UWB ranging and positioning precision in NLOS environments, a UWB positioning precision evaluation mechanism is introduced. Specifically, this paper theoretically analyzes the number of UWB devices and their geometric distribution to evaluate the positioning precision of UWB systems, and further optimizes the number and geometric distribution of UWB devices, to optimize the UWB positioning algorithm model to improve the positioning precision.

2. UWB AND INS POSITIONING ALGORITHMS AND ANALYSIS

The specific contents of this chapter are arranged as follows: Sections 2.1 and 2.2 introduce the algorithms of UWB positioning and INS respectively; Section 2.3 analyzes the UWB positioning accuracy, applies the Dilution of Precision (DOP) to the UWB positioning system, and gives the derivation of DOP; Section 2.4 introduces the Kalman filter algorithm that fuses INS and UWB information.

2.1 INS Mechanization

INS is currently one of the most important autonomous navigation systems. It uses 3D gyros and accelerometers to measure 3D angular velocities and specific forces, respectively. The measurements are used to continuously track the 3D attitude between the device's body frame (i.e., b-frame) and the navigation frame (i.e., n-frame). With the obtained attitude, the specific force vector can be transformed from the projection in the b-frame to that in the n-frame. Then, the gravity vector is added to the specific force to get the device acceleration vector

in the n-frame. Finally, the acceleration vector is integrated once and twice to determine the 3D velocity and position changes respectively (Groves, 2014). The specific process is shown in Figure 1.

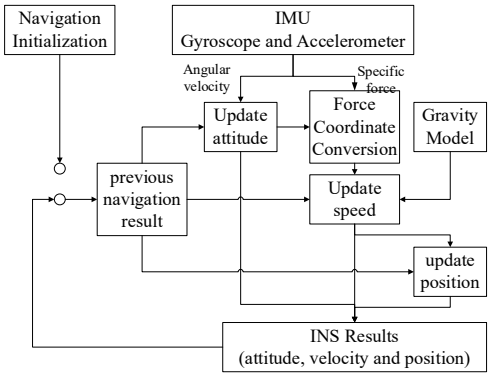

Figure 1. INS mechanization process.

2.2 UWB Positioning Algorithms

The basic principle of the UWB positioning system is similar to that of the GNSS positioning system. The UWB base station and mobile tag have a similar role to the satellite and receiver in the GNSS positioning system, respectively. The principle of geometric positioning can be used to complete indoor positioning. Therefore, the mathematical model for UWB positioning is

$$\tilde{\rho}_i = \sqrt{(x_i - x_u)^2 + (y_i - y_u)^2 + (z_i - z_u)^2} + b_\rho + \epsilon_{\rho,i} \quad (1)$$

where $(x_u,\ y_u\ ,z_u)$ is the node coordinate to be estimated; $(x_i,\ y_i,\ z_i)$ is the coordinate of the base station; $\tilde{\rho}_i$ is the measurement value of the distance from the node to the i-th base station; b_ρ is the bias in the distance measurement value; $\epsilon_{\rho,i}$ is the random error in the distance measurement.

After error perturbating and linearizing Equation (1), the ranging error model is

$$\Delta\rho_i = -\frac{x_i - \tilde{x}_u}{\tilde{r}_i}\Delta x_u - \frac{y_i - \tilde{y}}{\tilde{r}_i}\Delta y_u - \frac{z_i - \tilde{z}}{\tilde{r}_i}\Delta z_u + \Delta b_\rho + \epsilon_{\rho,i} \quad (2)$$

where

$$\Delta\rho_i = \rho_i - \tilde{\rho}_i$$
$$\Delta x_u = x_u - \tilde{x}_u$$
$$\Delta y_u = y_u - \tilde{y}_u$$
$$\Delta z_u = z_u - \tilde{z}_u$$
$$\Delta b_\rho = b_\rho - \tilde{b}_\rho$$
$$\tilde{r}_i = \sqrt{(\tilde{x}_u - x_i)^2 + (\tilde{y}_u - y_i)^2 + (\tilde{z}_u - z_i)^2}$$

~ stands for approximate distance.

After measuring the distance from the tag node to multiple base stations, the ranging error model can be constructed in the form of a matrix.

$$\mathbf{z} = \mathbf{H}\mathbf{x} + \mathbf{v} \quad (3)$$

where

$$\mathbf{z} = \begin{bmatrix} \Delta\rho_1 \\ \Delta\rho_2 \\ \vdots \\ \Delta\rho_{n_a} \end{bmatrix}$$

$$\mathbf{H} = \begin{bmatrix} -\frac{x_1 - \tilde{x}_u}{\tilde{r}_1} & -\frac{y_1 - \tilde{y}_u}{\tilde{r}_1} & -\frac{z_1 - \tilde{z}_u}{\tilde{r}_1} & 1 \\ -\frac{x_2 - \tilde{x}_u}{\tilde{r}_2} & -\frac{y_2 - \tilde{y}_u}{\tilde{r}_2} & -\frac{z_2 - \tilde{z}_u}{\tilde{r}_2} & 1 \\ \vdots & \vdots & \vdots & 1 \\ -\frac{z_{n_a} - \tilde{z}_u}{\tilde{r}_{n_a}} & -\frac{z_{n_a} - \tilde{z}_u}{\tilde{r}_{n_a}} & -\frac{z_{n_a} - \tilde{z}_u}{\tilde{r}_{n_a}} & 1 \end{bmatrix}$$

$$\mathbf{x} = \begin{bmatrix} \Delta x \\ \Delta y \\ \Delta z \\ \Delta b_\rho \end{bmatrix}$$

$$\mathbf{v} = \begin{bmatrix} \epsilon_{\rho,1} \\ \epsilon_{\rho,2} \\ \vdots \\ \epsilon_{\rho,n_a} \end{bmatrix}$$

The least square method can be used to estimate the error vector $\mathbf{x}$.

$$\mathbf{x} = (\mathbf{H}^T\mathbf{R}^{-1}\mathbf{H})^{-1}\mathbf{H}^T\mathbf{R}^{-1}\mathbf{z} \quad (4)$$

where

$$\mathbf{R} = [(\mathbf{v} - \mathrm{E}(\mathbf{v}))(\mathbf{v} - \mathrm{E}(\mathbf{v}))^T]$$

After $\mathbf{x}$ is estimated, it is fed back to the navigation state vector $\mathbf{X}$ and $\mathbf{x}$ is cleared, as shown in Equation (5). Keep iterating until the least square converges. One way to judge convergence is whether the modular value of the coordinate error vector in $\mathbf{x}$ is less than a preset threshold value. When the value is less than the threshold value, the least square method is judged to converge at this time and the iteration is finished. When the number of iterations exceeds the corresponding threshold value, there is still no convergence, then the solution of the position least square method fails. Navigation state vector $\mathbf{X}$ is the position coordinate to be estimated, and the initial value can be set to the positioning result at the last time.

$$\mathbf{X} = \mathbf{X} + \mathbf{x},\ \mathbf{x} = 0 \quad (5)$$

2.3 Analysis of UWB Positioning Accuracy

DOP describes the geometric strength of the configuration of the visible satellite on the GPS accuracy (Tahsin M et al., 2015). The UWB positioning system is similar to the GNSS positioning system. Thus, in this paper, DOP is applied to the UWB positioning system. The number and geometric distribution of UWB base stations and the DOP value are theoretically analyzed. The DOP value is further used to evaluate the positioning precision of the UWB system and optimize its base station number and geometry, to optimize the parameter settings of the positioning algorithm to achieve a better indoor positioning solution. It can be seen from Table 1 that the smaller the DOP value, the better the geometric distribution.

DOP Value	Ratings
1-2	Ideal
2-4	Excellent
4-6	Good
6-8	Moderate
8-20	Fair
20-50	Poor

Table 1. DOP ratings (Tahsin M et al., 2015).

If the random error term of Equation (3) is ignored

$$\mathbf{x} = (\mathbf{H}^T\mathbf{H})^{-1}\mathbf{H}^T\mathbf{z} \tag{6}$$

Then the covariance matrix of $\mathbf{x}$ is

$$\begin{aligned}\mathrm{cov}(\mathbf{x}) &= \mathrm{E}(\mathbf{x}\mathbf{x}^T)\\ &= \mathrm{E}((\mathbf{H}^T\mathbf{H})^{-1}\mathbf{H}^T\mathbf{z}\mathbf{z}^T\mathbf{H}(\mathbf{H}^T\mathbf{H})^{-T})\\ &= (\mathbf{H}^T\mathbf{H})^{-1}\mathbf{H}^T\mathbf{z}\mathbf{z}^T\mathbf{H}(\mathbf{H}^T\mathbf{H})^{-T}\\ &= (\mathbf{H}^T\mathbf{H})^{-1}\mathbf{H}^T\mathrm{cov}(\mathbf{z})\mathbf{H}(\mathbf{H}^T\mathbf{H})^{-T}\end{aligned} \tag{7}$$

$\mathrm{cov}(\mathbf{z})$ represents the ranging accuracy of UWB. Here it is assumed that they all have the same variance as σ_n.

$$\begin{aligned}\mathrm{cov}(\mathbf{x}) &= \mathrm{E}(\mathbf{x}\mathbf{x}^T)\\ &= \sigma_n^2(\mathbf{H}^T\mathbf{H})^{-T}\\ &= \sigma_n^2(\mathbf{H}^T\mathbf{H})^{-1}\end{aligned} \tag{8}$$

Let $\mathbf{Q}_p = (\mathbf{H}^T\mathbf{H})^{-1}$,then

$$\begin{aligned}&\begin{bmatrix}\sigma_x^2 & \mathrm{cov(x,y)} & \mathrm{cov(x,z)} & \mathrm{cov(x,b)}\\ \mathrm{cov(y,x)} & \sigma_y^2 & \mathrm{cov(y,z)} & \mathrm{cov(y,b)}\\ \mathrm{cov(z,x)} & \mathrm{cov(z,y)} & \sigma_z^2 & \mathrm{cov(z,b)}\\ \mathrm{cov(b,x)} & \mathrm{cov(b,y)} & \mathrm{cov(b,z)} & \sigma_b^2\end{bmatrix}\\ &= \sigma_n^2\begin{bmatrix}G_{xx} & G_{xy} & G_{xz} & G_{xb}\\ G_{yx} & G_{yy} & G_{yz} & G_{yb}\\ G_{zx} & G_{zy} & G_{zz} & G_{zb}\\ G_{bx} & G_{by} & G_{bz} & G_{bb}\end{bmatrix}\end{aligned} \tag{9}$$

We can write,

$$\begin{bmatrix}\sigma_x\\ \sigma_y\\ \sigma_z\\ \sigma_b\end{bmatrix} = \sigma_n\begin{bmatrix}\sqrt{G_{xx}}\\ \sqrt{G_{yy}}\\ \sqrt{G_{zz}}\\ \sqrt{G_{bb}}\end{bmatrix} \tag{10}$$

Then, the DOP values in the east, north, and elevation directions can be obtained as

$$\begin{aligned}DOP_E &= \sqrt{G_{xx}}\\ DOP_N &= \sqrt{G_{yy}}\\ DOP_D &= \sqrt{G_{zz}}\end{aligned} \tag{11}$$

Furthermore, the DOP values for the horizon, vertical, and 3D directions are calculated as

$$\begin{aligned}DOP_{hor} &= \sqrt{G_{xx}+G_{yy}}\\ DOP_{ver} &= \sqrt{G_{zz}}\\ DOP_{\rho} &= \sqrt{G_{xx}+G_{yy}+G_{zz}}\end{aligned} \tag{12}$$

The positioning precision of UWB is affected by the combined effect of measurement error and the geometric distribution of UWB base stations. Measurement errors and deviations can be expressed as the User Equivalent Range Errors (UERE). If the measurement errors of all UWB base stations are the same and independent, the UERE definition can be the square root of the various errors and deviations. Multiplying UERE by the DOP_p value gives the expected precision of UWB positioning, as shown in Equation (13) (Langley, 1999)

$$UWB\ Position\ accuracy = UERE \times DOP_p \tag{13}$$

2.4 INS and UWB Information Fusion

In this paper, Kalman filter is used to fuse the information output by UWB and INS. The state equation and measurement equation are

$$\begin{cases}\delta x_{k+1} = \mathbf{\Phi}_{k+1,k}\delta x_k + \omega_k\\ z_{k+1} = \mathbf{H}_{k+1}\delta x_{k+1} + \nu_{k+1}\end{cases} \tag{14}$$

where (Farrell and Barth, 1999)

$$\mathbf{\Phi}_{k+1,k} = \begin{bmatrix}I_3 & T_sI_3 & 0_{3,3} & 0_{3,3} & 0_{3,3}\\ 0_{3,3} & I_3 & T_s[C_b^n s_k]\times & T_sC_b^n & 0_{3,3}\\ 0_{3,3} & 0_{3,3} & I_3 & 0_{3,3} & -T_sC_b^n\\ 0_{3,3} & 0_{3,3} & 0_{3,3} & I_3 & 0_{3,3}\\ 0_{3,3} & 0_{3,3} & 0_{3,3} & 0_{3,3} & I_3\end{bmatrix}$$

$$\delta x_k = [\delta p_k\ \ \delta v_k\ \ \epsilon_k\ \ a_b\ \ \omega_b]^T$$

$$\mathbf{H}_{k+1} = [I_3\ \ 0_{3,12}]$$

where δp_k, δv_k, ϵ_k, a_b, ω_b is the error of position, velocity, attitude, accelerometer bias, and gyro bias, respectively; s_k is the acceleration information collected by the IMU; T_s is the time interval of the IMU output; ω_k is the system noise; ν_{k+1} is the measurement of UWB positioning noise. The prediction formula of the Kalman filter is

$$\begin{cases}\delta x_{k+1}^- = \mathbf{\Phi}_{k+1,k}\delta x\\ \mathbf{P}_{k+1}^- = \mathbf{\Phi}_{k+1}\mathbf{P}_k\mathbf{\Phi}_{k+1,k}^T + \mathbf{Q}_k\end{cases} \tag{15}$$

The measurement equation is

$$\begin{cases}\mathbf{K}_{k+1} = \mathbf{P}_{k+1}^-\mathbf{H}_{k+1}^T[\mathbf{H}_{k+1}\mathbf{P}_{k+1}^-\mathbf{H}_{k+1}^T + \mathbf{R}_{k+1}]^{-1}\\ \delta x_{k+1} = \delta x_{k+1}^- + \mathbf{K}_{k+1}[z_{k+1} - \mathbf{H}_{k+1}\delta x_{k+1}^-]\\ \mathbf{P}_{k+1} = [\mathbf{I} - \mathbf{K}_{k+1}\mathbf{H}_{k+1}]\mathbf{P}_{k+1}^-\end{cases} \tag{16}$$

where $\mathbf{P}$ is the covariance matrix of the state vector δx; $\mathbf{K}$ is the gain matrix of the Kalman filter; $\mathbf{Q}$ and $\mathbf{R}$ are the system noise covariance matrix and the observation noise covariance matrix, respectively; the subscripts k and $k+1$ represent the times of t_k and t_{k+1}, and the superscript '-' indicates that the item is a forecast item.

3. EXPERIMENT AND RESULT ANALYSIS

3.1 Simulation of DOP value

In the UWB positioning system, the DOP value depends on the geometric distribution of the base stations. In this paper, the exhaustive method is used to obtain the DOP simulation results of setting four base stations in a 25 m * 20 m scene and find the base station arrangement with the smallest average DOP value. Figures 2 and 3 show the DOP distributions of two different base station arrangements of 'solution 1' and 'solution 2'. The DOP value distribution diagram shown in Figure 2 is that four UWB base stations are arranged in the four corners of the scene, and its DOP values are the smallest, which has the best geometric distribution.

The UWB positioning is simulated by the base station arrangement of 'solution 1', and the Equation (13) is verified. It is assumed here that the measurement errors of all UWB base stations are the same and independent. Afterward, four test points and four UERE values are set to test the relation between DOP and positioning accuracy. For each combination of test point and UERE, 100,000 simulations are run, the RMS value of the error is calculated. The statistical results are shown in Table 2.

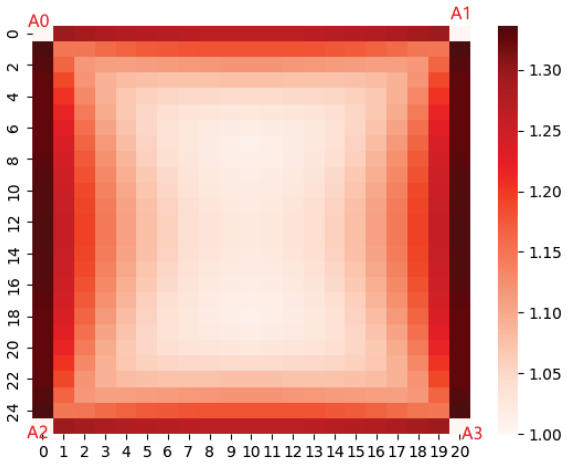

Figure 2. DOP value distribution for 'solution 1'.

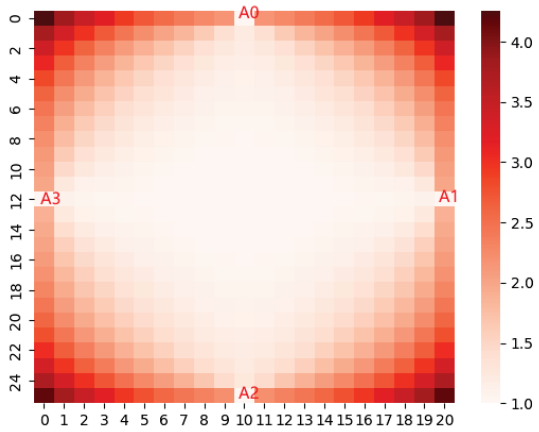

Figure 3. DOP value distribution for 'solution 2'.

It can be seen from Figure 4 that the positioning accuracy of UWB varies with the changes of UERE and DOP values. Under a certain UERE, with the increase of the DOP value, the RMS value of the positioning error will also increase; at a certain test point, the RMS of the positioning error will increase with the increase of the UERE. As can be seen from Table 2, for a certain test point, such as test point (12.06, 10.36), its DOP value is 1.025, and when the UERE is 0.1, 0.5, and 1, its positioning error RMS is 0.1077, 0.5393 and 1.0788 respectively, but the ratio of RMS to UERE is 1.0770, 1.0786, 1.0788, no matter what its UERE and RMS values are, the ratio of RMS to UERE is almost equal, and it is very close to the DOP value of the test point.

UERE /m	Test point/m	DOP	Position error RMS/m	$\frac{\text{RMS}}{\text{UERE}}$
0	(12.06, 10.36)	1.025	1.776e-15	xxx
	(9.80, 2.10)	1.182	1.831e-15	xxx
	(1.78, 0.30)	1.258	1.955e-15	xxx
	(10.78, 19.30)	1.277	3.552e-15	xxx
0.1	(12.06, 10.36)	1.025	0.1077	1.0770
	(9.80, 2.10)	1.182	0.1097	1.0970
	(1.78, 0.30)	1.258	0.1212	1.2120
	(10.78, 19.30)	1.277	0.1305	1.3050
0.5	(12.06, 10.36)	1.025	0.5393	1.0786
	(9.80, 2.10)	1.182	0.5473	1.0946
	(1.78, 0.30)	1.258	0.6051	1.2102
	(10.78, 19.30	1.277	0.6520	1.3040
1	(12.06, 10.36)	1.025	1.0788	1.0788
	(9.80, 2.10)	1.182	1.1005	1.1005
	(1.78, 0.30)	1.258	1.2143	1.2143
	(10.78, 19.30)	1.277	1.3092	1.3092

Table 2. RMS of position errors with four test points and UERE values.

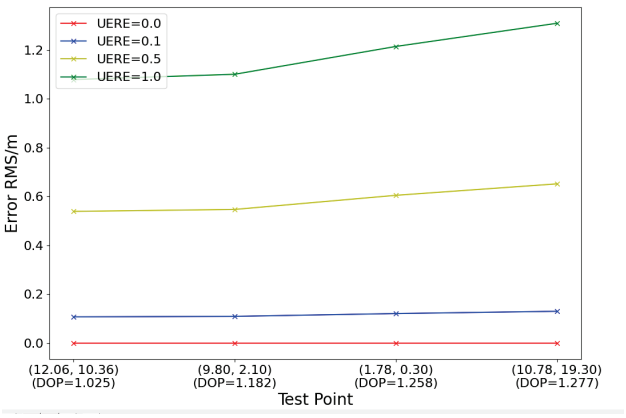

Figure 4. Positioning error RMS at four simulated results.

3.2 Experiment of UWB

The test environment of the UWB positioning system is a 25.0 m * 20.0 m outdoor area with a wide field of view. The test environment is shown in Figure 5. When tested outdoors, there is almost no obstruction between the UWB base station and the tag node. First, arrange four UWB base stations in the area. The arrangement of 'solution 1' is to place the base station in the four corners of the scene, and 'solution 2' is to place the base station in the middle of the four sides of the scene. After calculating, the geometric distribution solution of 'solution 1' is better than that of 'solution 2'. The DOP value distributions are shown in Figure 2 and Figure 3.

During the experiment, the UWB tag was attached to the chest, and then the walking test was performed. UWB tag installation

as shown in Figure 6. Figure 7 shows the comparison between the calculated walking trajectories and the real trajectories under these two different base station arrangement solutions. The reference trajectories are obtained by setting the traveling trajectories on the area in advance and measuring them at the corners of the trajectories. As can be seen from Figure 7, the trajectories obtained by these two UWB base station arrangements are not much different, the positioning results are continuous and close to the real trajectory, and the positioning precision is at the decimetre-level.

Figure 5. Test environment of the UWB positioning system.

Figure 6. UWB tag installation.

This is because the average DOP values of the two base station solutions are 1.129 and 1.556, which are both between 1 and 2. According to the DOP ratings in Table 1, these two solutions are ideal. In addition, these two trajectories were completed in two experiments respectively. During the process of traveling, there may be slight deviations in the trajectories of people walking, and there may also be ranging errors when measuring the corner points, resulting in the actual walking track and the reference track may be different, and there is a certain error. Therefore, the positioning precision of 'solution 1' is not significantly better than that of 'solution 2'.

However, in an indoor environment, the positioning performance may be affected by NLOS and multipath due to various occlusions such as walls, resulting in a larger ranging error and a smaller maximum ranging distance. This paper chooses the positioning method of UWB/INS to reduce the influence of NLOS.

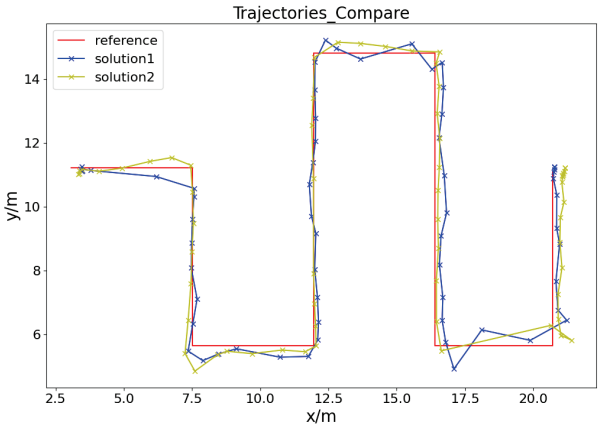

Figure 7. Comparison of the reference trajectory and the trajectory obtained by the two base station arrangements of 'solution 1' and 'solution 2'.

3.3 Experiment of UWB/INS

In this paper, the indoor test is carried out through experiment/simulation. During the experiment, the 'Weartrack' module is used to provide the true value of the position reference. The 'Weartrack' module is a small low-power wearable positioning system, which was developed by the MOTION team of LIESMARS of Wuhan University and the i2Nav team of the Satellite Navigation and Positioning Technology Research Centre of Wuhan University. The system can achieve decimeter-level positioning precision after sufficient landmark point correction and forward-backward smoothing.

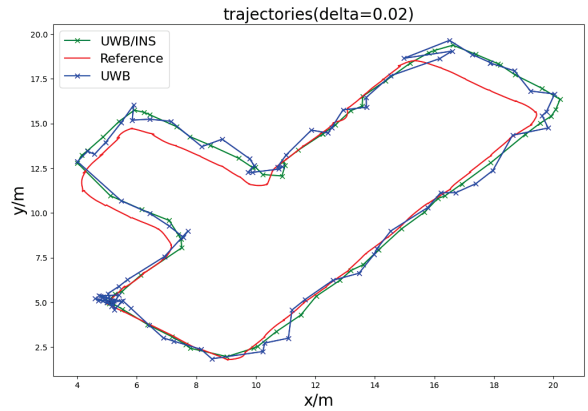

Figure 8. Comparison of reference trajectory, UWB trajectory, and UWB/INS integration trajectory when $\delta_0 = \delta_1 = \delta_2 = 0.02$ (δ_0, δ_1, δ_2 are the diagonal elements of the observation noise covariance matrix).

The position provided by the 'Weartrack' module is used to calculate the true value of the distance from the tag node to the four base stations. Then, NLOS errors are added to the true distance value to simulate the actual distance measurement value. Finally, simulated distance measurement values are used to perform the positioning solution. The positioning results are compared with the reference truth of the positioning results provided by 'Weartrack' to evaluate the positioning precision.

To verify the influence of the uncertainty of UWB positioning results on UWB/INS positioning, this paper sets two different

constant values for the observation noise covariance matrix $\mathbf{R}$, which has components of

$$\mathbf{R} = \begin{bmatrix} \delta_0^2 & 0 & 0 \\ 0 & \delta_1^2 & 0 \\ 0 & 0 & \delta_2^2 \end{bmatrix}$$

Here $\delta_0 = \delta_1 = \delta_2 = 0.02$ and $\delta_0 = \delta_1 = \delta_2 = 0.2$ are set. The trajectory figure and error figure of the two observation noise covariance matrices are shown in Figures 8 to 11.

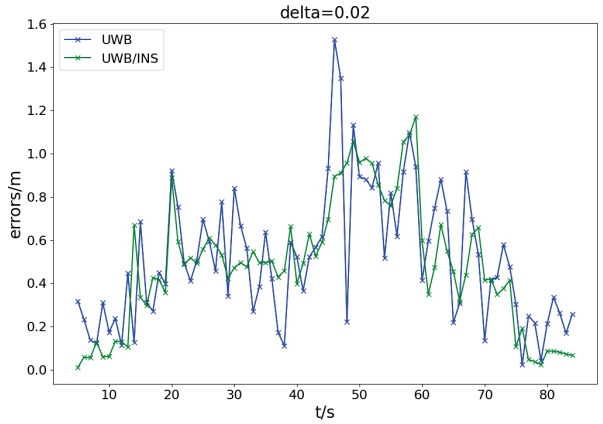

Figure 9. Comparison of the positioning error of UWB and the positioning error of UWB/INS integration when $\delta_0 = \delta_1 = \delta_2 = 0.02$ (δ_0, δ_1, δ_2 are the diagonal elements of the observation noise covariance matrix).

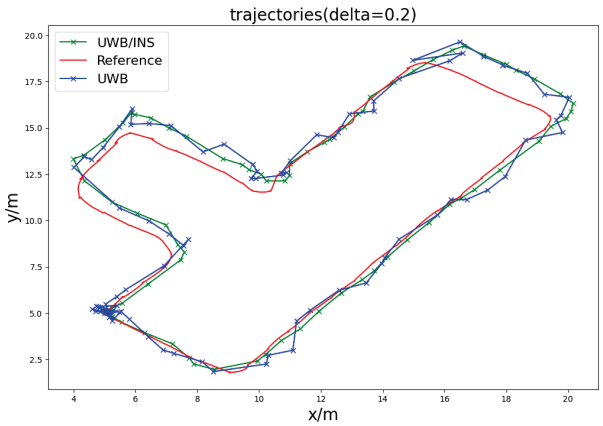

Figure 10. Comparison of reference trajectory, UWB trajectory, and UWB/INS integration trajectory when $\delta_0 = \delta_1 = \delta_2 = 0.2$ (δ_0, δ_1, δ_2 are the diagonal elements of the observation noise covariance matrix).

It can be seen from Figures 8 to 11 that after using UWB/INS integration, the localization error is reduced, and the trajectory is smoother. The combined positioning results of the two observation noise covariance matrices with different constants are compared, as shown in Table 3. Without the influence of NLOS, using UWB/INS only reduced the MEAN and RMS of errors by only 2-4 cm. By contrast, under the influence of NLOS, the maximum positioning error of UWB positioning reaches 1.5 m; after using UWB/INS, the maximum error is reduced by nearly 0.4 m, with an accuracy improvement of 26.7 %, which has a certain inhibitory effect on NLOS.

The indoor locating scene in the actual application, because the influence of the UWB base station to tag node won't be the same, some obstructions between the base station and tag caused the ranging error is bigger, the reliability of the base station to drop. Thus, in the UWB positioning results are estimates, should consider the weight of each base station's influence on the tag node. In addition, the observed noise covariance matrix should change with the movement of pedestrians at different positions. When UWB is affected by NLOS or multipath, the reliability of UWB positioning results is weakened. At this time, the observation noise covariance matrix should be set larger. This reflects the importance of setting the observation noise covariance matrix for integrated navigation performance.

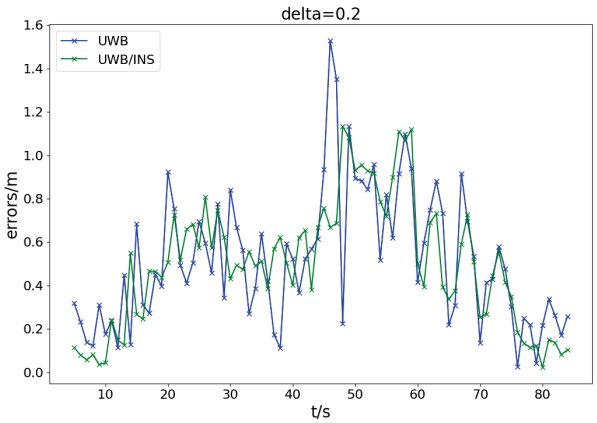

Figure 11. Comparison of the positioning error of UWB and the positioning error of UWB/INS integration when $\delta_0 = \delta_1 = \delta_2 = 0.2$ (δ_0, δ_1, δ_2 are the diagonal elements of the observation noise covariance matrix).

	STD/m	MEAN/m	RMS/m	MAX/m
$\delta_{0,1,2} = 0.02$	0.2946	0.4813	0.5643	1.1713
$\delta_{0,1,2} = 0.2$	0.2892	0.4986	0.5764	1.1331
UWB	0.3071	0.5172	0.6015	1.5283

Table 3. Statistical values of position errors for UWB/INS integration with various measurement noises.

4. CONCLUSIONS

Although UWB positioning is a highly precise method, its precision is affected by bad factors such as NLOS. In this paper, DOP is applied to the UWB positioning system, and a set of calculation processes of UWB positioning precision and reliability is proposed. Through theoretical analysis and simulation, a model of the influence of base station geometric distribution on UWB positioning precision in the test scene is established. In the indoor positioning, it provides a reference for the arrangement of the UWB base station. As shown in Table 3, the combined positioning method of UWB/INS has reduced the STD, MEAN, RMS, and MAX of the positioning error compared with the positioning method that only uses UWB technology, which reduces the influence of NLOS and improves the positioning precision and robustness. The maximum error is reduced by nearly 0.4 m, with an accuracy improvement of 26.7 %. However, the STD of position errors is only reduced by 1-2 cm, while MEAN and RMS are both reduced by 2-3 cm. This is because the noise covariance matrix here is set to a

constant value, so the positioning accuracy does not improve much. This also reflects the importance of the setting of the observation noise covariance matrix to the UWB/INS positioning system.

ACKNOWLEDGEMENTS

This work was supported in part by the Major Basic Research Project (5140503A0301), the National Natural Science Foundation of China (42174050), the Provincial and Municipal "Double First-Class" Construction Project (600460035), and the Hubei Luojia Laboratory Special Fund.

REFERENCES

Balland P A. Proximity and the evolution of collaboration networks: evidence from research and development projects within the global navigation satellite system (GNSS) industry[J]. Regional studies, 2012, 46(6): 741-756.

Poulose A, Eyobu O S, Han D S. An indoor position-estimation algorithm using smartphone IMU sensor data[J]. Ieee Access, 2019, 7: 11165-11177.

Park C, Rappaport T S. Short-range wireless communications for next-generation networks: UWB, 60 GHz millimeter-wave WPAN, and ZigBee[J]. IEEE Wireless Communications, 2007, 14(4): 70-78.

El-Sheimy N, Li Y. Indoor navigation: State of the art and future trends[J]. Satellite Navigation, 2021, 2(1): 1-23.

Groves P. D, "Principles of GNSS, inertial, and multisensor integrated navigation systems, 2nd edition [Book review]," in IEEE Aerospace and Electronic Systems Magazine, vol. 30, no. 2, pp. 26-27, Feb. 2015, doi: 10.1109/MAES.2014.14110.

Tahsin M, Sultana S, Reza T, et al. Analysis of DOP and its preciseness in GNSS position estimation[C]//2015 International conference on electrical engineering and information communication technology (ICEEICT). IEEE, 2015: 1-6.

Langley R.B. , "Dilution of Precision," GPS World, pp. 52-59, 1999.

Y.B.S. Srilatha Indira Dutt, G.Sasi Bhushana Rao, S.Swapna Rani, Swama Ravindra Babu, Rajkumar Goswami and Ch. Usha Kumari, "Investigation of GDOP for Precise user Position Computation with all Satellites in view and Optimum four Satellite Configurations," J. Ind. Geophys. Union, vol. 13, noJ, pp. 139-148, July 2009.

Teunissen P J G. Quality control and GPS[M]//GPS for Geodesy. Springer, Berlin, Heidelberg, 1998: 271-318.

Farrell J, Barth M. The global positioning system and inertial navigation[M]. New York: Mcgraw-hill, 1999.

Zwirello L, Ascher C, Trommer G F, et al. Study on UWB/INS integration techniques[C]//2011 8th Workshop on Positioning, Navigation and Communication. IEEE, 2011: 13-17.